

Introduction

Experimental analysis

Results

Interpretation

Methods

Summary & Conclusions

Back-up

Measurement and QCD analysis of double-differential inclusive jet cross sections in proton-proton collisions at $\sqrt{s} = 13$ TeV

Computational Discussions with Coffee and Sweets

Patrick L.S. CONNOR

Universität Hamburg

5 April 2022

Bundesministerium
für Bildung
und Forschung

UH



Introduction

Reminder

Goal

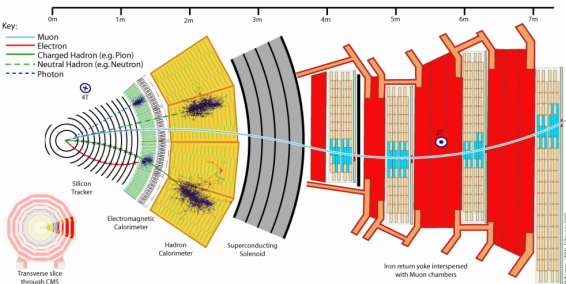
Motivation

Experimental data

Introduction**Reminder****Goal****Motivation****Experimental data****Experimental analysis****Results****Interpretation****Methods****Summary & Conclusions****Back-up**

Reminder

LHC & CMS



Introduction

Reminder

Goal

Motivation

Experimental data

Experimental analysis

Results

Interpretation

Methods

Summary & Conclusions

Back-up



$$\begin{aligned}
 1 \quad & -\frac{1}{2}\partial_\nu g^a_\mu \partial_\nu g^a - g_s f^{abc} \partial_\mu g^a g^b_\nu - \frac{1}{4}g_s^2 f^{abc} f^{ade} g^b_\mu g^c_\nu g^d_\nu + \\
 & \frac{1}{2}ig_w^2 (\tilde{q}^\mu q^\nu) g^a_\mu + \bar{G}^a \partial^2 G^a + g_s f^{abc} \partial_\mu G^a G^b g^c_\mu - \partial_\nu W^+_\mu \partial_\nu W^-_\\mu - \\
 2 \quad & M^2 W^+_\mu W^-_\mu - \frac{1}{2}\partial_\nu Z^0_\mu \partial_\nu Z^0_\mu - \frac{1}{2c_w^2} M^2 Z^0_\mu Z^0_\mu - \frac{1}{2}\partial_\mu A_\mu A_\mu - \frac{1}{2}\partial_\mu H \partial_\mu H - \\
 & \frac{1}{2}m_h^2 H^2 - \partial_\mu \phi^+ \partial_\mu \phi^- - M^2 \phi^+ \phi^- - \frac{1}{2}\partial_\mu \phi^0 \partial_\mu \phi^0 - \frac{1}{2c_w^2} M \phi^0 \phi^0 - \beta_h [\frac{2M^2}{g^2} + \\
 & \frac{2M}{g} H + \frac{1}{2}(H^2 + \phi^0 \phi^0 + 2\phi^+ \phi^-)] + \frac{2M^4}{g^2} \alpha_h - ig c_w [\partial_\nu Z^0_\mu (W^+_\mu W^-_\\mu - \\
 & W^+_\\mu W^-_\\mu) - Z^0_\nu (W^+_\mu \partial_\nu W^-_\\mu - W^-_\\mu \partial_\nu W^+_\mu) + Z^0_\mu (W^+_\nu \partial_\nu W^-_\\mu - \\
 & W^-_\\nu \partial_\nu W^+_\mu)] - ig s_w [\partial_\nu A_\mu (W^+_\mu W^-_\\nu - W^-_\\mu W^+_\mu) - A_\nu (W^+_\mu \partial_\nu W^-_\\mu - \\
 & W^-_\\mu \partial_\nu W^+_\mu) + A_\mu (W^+_\nu \partial_\nu W^-_\\mu - W^-_\\nu \partial_\nu W^+_\mu)] - \frac{1}{2}g^2 W^+_\mu W^-_\\mu W^+_\nu W^-_\\nu + \\
 & \frac{1}{2}g^2 W^+_\mu W^-_\\nu W^+_\nu W^-_\\nu + g^2 c_w^2 (Z^0_\mu W^+_\mu Z^0_\nu W^-_\\nu - Z^0_\mu Z^0_\nu W^+_\nu W^-_\\nu) + \\
 & g^2 s_w^2 (A_\mu W^+_\mu A_\nu W^-_\\nu - A_\mu A_\nu W^+_\nu W^-_\\nu) + g^2 s_w c_w [A_\mu Z^0_\nu (W^+_\mu W^-_\\nu - \\
 & W^+_\nu W^-_\\mu) - 2A_\mu Z^0_\nu W^+_\nu W^-_\\nu] - g\alpha [H^3 + H\phi^0 \phi^0 + 2H\phi^+ \phi^-] - \\
 & \frac{1}{8}g^2 \alpha_h [H^4 + (\phi^0)^4 + 4(\phi^+ \phi^-)^2 + 4(\phi^0 \phi^0)^2 \phi^+ \phi^- + 4H^2 \phi^+ \phi^- + 2(\phi^0)^2 H^2] - \\
 & gMW^+_\mu W^-_\\mu H - \frac{1}{2}g \frac{M}{c_w^2} Z^0_\mu Z^0_\nu H - \frac{1}{2}ig [W^+_\mu (\phi^0 \partial_\mu \phi^- - \phi^- \partial_\mu \phi^0) - \\
 & W^-_\\mu (\phi^0 \partial_\mu \phi^+ - \phi^- \partial_\mu \phi^0)] + \frac{1}{2}g [W^+_\mu (H \partial_\mu \phi^- - \phi^- \partial_\mu H) - W^-_\\mu (H \partial_\mu \phi^+ - \\
 & \phi^+ \partial_\mu H)] + \frac{1}{2}g \frac{1}{c_w^2} (Z^0_\mu (H \partial_\mu \phi^0 - \phi^0 \partial_\mu H) - ig \frac{s_w^2}{c_w} M Z^0_\mu (W^+_\mu \phi^- - W^-_\\mu \phi^+) + \\
 & ig s_w M A_\mu (W^+_\mu \phi^- - W^-_\\mu \phi^+) - ig \frac{1-2c_w^2}{2c_w^2} Z^0_\mu (\phi^+ \partial_\mu \phi^- - \phi^- \partial_\mu \phi^+) + \\
 & ig s_w A_\mu (\phi^+ \partial_\mu \phi^- - \phi^- \partial_\mu \phi^+) - \frac{1}{4}g^2 W^+_\mu W^-_\\mu [H^2 + (\phi^0)^2 + 2\phi^+ \phi^-] - \\
 & \frac{1}{4}g^2 \frac{1}{c_w^2} Z^0_\mu Z^0_\nu [H^2 + (\phi^0)^2 + 2(2s_w^2 - 1)^2 \phi^+ \phi^-] - \frac{1}{2}g^2 \frac{s_w^2}{c_w^2} Z^0_\mu \phi^0 (W^+_\mu \phi^- + \\
 & W^-_\\mu \phi^+) - \frac{1}{2}ig^2 \frac{s_w^2}{c_w^2} Z^0_\mu H (W^+_\mu \phi^- - W^-_\\mu \phi^+) + \frac{1}{2}g^2 s_w A_\mu \phi^0 (W^+_\mu \phi^- + \\
 & W^-_\\mu \phi^+) + \frac{1}{2}ig^2 s_w A_\mu H (W^+_\mu \phi^- - W^-_\\mu \phi^+) - g^2 \frac{s_w^2}{c_w^2} (2c_w^2 - 1) Z^0_\mu A_\mu \phi^+ \phi^- - \\
 & g^2 s_w^2 A_\mu A_\mu \phi^+ \phi^- - \bar{e}^\lambda (\gamma \partial + m_e^\lambda) e^\lambda - \bar{\nu}^\lambda \gamma^\mu \partial \bar{\nu}^\lambda - \bar{u}_j^\lambda (\gamma \partial + m_u^\lambda) u_j^\lambda - \\
 3 \quad & d_j^\lambda (\gamma \partial + m_d^\lambda) d_j^\lambda + ig s_w A_\mu [-(\bar{e}^\lambda \gamma^\mu e^\lambda) + \frac{2}{3}(\bar{u}_j^\lambda \gamma^\mu u_j^\lambda) - \frac{1}{3}(\bar{d}_j^\lambda \gamma^\mu d_j^\lambda)] + \\
 & \frac{ig}{4c_w} Z^0_\mu [(\bar{\nu}^\lambda \gamma^\mu (1 + \gamma^5) \nu^\lambda) + (\bar{e}^\lambda \gamma^\mu (4s_w^2 - 1 - \gamma^5) e^\lambda) + (\bar{u}_j^\lambda \gamma^\mu (\frac{1}{2}s_w^2 - \\
 & 1 - \gamma^5) u_j^\lambda) + (d_j^\lambda \gamma^\mu (1 - \frac{3}{2}s_w^2 - \gamma^5) d_j^\lambda)] + \frac{ig}{\sqrt{2}} W_\mu^+ [(\bar{\nu}^\lambda \gamma^\mu (1 + \gamma^5) e^\lambda) + \\
 & (\bar{u}_j^\lambda \gamma^\mu (1 + \gamma^5) C_{\lambda\kappa} d_j^\kappa)] + \frac{ig}{2\sqrt{2}} W_\mu^- [(\bar{e}^\lambda \gamma^\mu (1 + \gamma^5) \nu^\lambda) + (d_j^\lambda C_{\lambda\kappa}^\dagger \gamma^\mu (1 + \\
 & \gamma^5) u_j^\lambda)] + \frac{ig}{2\sqrt{2}} \frac{m_e^2}{M} [-\phi^+ (\bar{\nu}^\lambda (1 - \gamma^5) e^\lambda) + \phi^- (\bar{e}^\lambda (1 + \gamma^5) \nu^\lambda)] - \\
 4 \quad & \frac{g}{M} \frac{m_\lambda^2}{M} [H (\bar{e}^\lambda e^\lambda) + i\phi^0 (\bar{e}^\lambda \gamma^5 e^\lambda)] + \frac{ig}{2M\sqrt{2}} \phi^+ [-m_d^\kappa (\bar{u}_j^\lambda C_{\lambda\kappa} (1 - \gamma^5) d_j^\kappa) + \\
 & m_u^\kappa (\bar{u}_j^\lambda C_{\lambda\kappa} (1 + \gamma^5) d_j^\kappa) + \frac{ig}{2M\sqrt{2}} \phi^- [m_d^\kappa (\bar{d}_j^\lambda C_{\lambda\kappa}^\dagger (1 + \gamma^5) u_j^\kappa) - m_u^\kappa (\bar{d}_j^\lambda C_{\lambda\kappa}^\dagger (1 - \\
 & \gamma^5) u_j^\kappa]] - \frac{g}{M} \frac{m_\lambda^2}{M} H (\bar{u}_j^\lambda u_j^\lambda) - \frac{g}{M} \frac{m_\lambda^2}{M} H (\bar{d}_j^\lambda d_j^\lambda) + \frac{ig}{M} \frac{m_\lambda^2}{M} \phi^0 (\bar{u}_j^\lambda \gamma^5 u_j^\lambda) - \\
 & \frac{ig}{2} \frac{m_\lambda^2}{M} \phi^0 (\bar{d}_j^\lambda \gamma^5 d_j^\lambda) + \bar{X}^+ (\partial^2 - M^2) X^+ + \bar{X}^- (\partial^2 - M^2) X^- + \bar{X}^0 (\partial^2 - \\
 & M^2) X^0 + \bar{Y} \partial^2 Y + ig c_w W_\mu^+ (\partial_\mu \bar{X}^0 X^- - \partial_\mu \bar{X}^0 X^0) + ig s_w W_\mu^+ (\partial_\mu \bar{Y} X^- - \\
 & \partial_\mu \bar{Y} X^0) + ig c_w Z_\mu^0 (\partial_\mu \bar{X}^+ X^+ - \partial_\mu \bar{X}^- X^-) + ig s_w A_\mu (\partial_\mu \bar{X}^+ X^+ - \\
 & \partial_\mu \bar{X}^- X^-) - \frac{1}{2}g M [\bar{X}^+ X^0 H + \bar{X}^- X^- H + \frac{1}{c_w^2} \bar{X}^0 X^0 H] + \\
 & \frac{1-2c_w^2}{2c_w^2} ig M [\bar{X}^+ X^0 \phi^+ - \bar{X}^- X^0 \phi^-] + \frac{1}{2c_w^2} ig M [\bar{X}^0 X^- \phi^+ - \bar{X}^0 X^+ \phi^-] + \\
 & ig M s_w [\bar{X}^0 X^- \phi^+ - \bar{X}^0 X^+ \phi^-] + \frac{1}{2}ig M [\bar{X}^+ X^+ \phi^0 - \bar{X}^- X^- \phi^0]
 \end{aligned}$$

Reminder

Standard Model

Lagrangian of the SM

- 1 QCD sector
- 2 EW sector for boson-only interactions
- 3 EW sector for boson-fermions interactions
- 4 (Higgs ghosts)
- 5 (Faddeev-Popov ghosts)



$$\begin{aligned}
 1 & -\frac{1}{2}\partial_\nu g^a_\mu \partial_\nu g^a - g_s f^{abc} \partial_\mu g^a g^b g^c_\nu - \frac{1}{4}g_s^2 f^{abc} f^{ade} g^b_\mu g^c_\nu g^d_\nu g^e + \\
 & \frac{1}{2}ig_w^2 (\tilde{q}^\mu q^\nu q^\rho) g^a_\mu + \bar{G}^a \partial^2 G^a + g_s f^{abc} \partial_\mu G^a G^b g^c_\mu - \partial_\nu W^+_\mu \partial_\nu W^-_ - \\
 2 & M^2 W^+_\mu W^-_\mu - \frac{1}{2}\partial_\nu Z^0_\mu \partial_\nu Z^0_\mu - \frac{1}{2c_w^2} M^2 Z^0_\mu Z^0_\mu - \frac{1}{2}\partial_\mu A_\mu A_\mu - \frac{1}{2}\partial_\mu H \partial_\mu H - \\
 & \frac{1}{2}m_h^2 H^2 - \partial_\mu \phi^+ \partial_\mu \phi^- - M^2 \phi^+ \phi^- - \frac{1}{2}\partial_\mu \phi^0 \partial_\mu \phi^0 - \frac{1}{2c_w^2} M \phi^0 \phi^0 - \beta_h [\frac{2M^2}{g^2} + \\
 & \frac{2M}{g} H + \frac{1}{2}(H^2 + \phi^0 \phi^0 + 2\phi^+ \phi^-)] + \frac{2M^4}{g^2} \alpha_h - ig c_w [\partial_\nu Z^0_\mu (W^+_\mu W^-_ - \\
 & W^+_ \mu W^-_) - Z^0_\nu (W^+_\mu \partial_\nu W^-_ - W^-_\mu \partial_\nu W^+)] + Z^0_\mu (W^+_\mu \partial_\nu W^-_ - \\
 & W^-_\mu \partial_\nu W^+_\mu)] - ig s_w [\partial_\nu A_\mu (W^+_\mu W^-_ - W^-_\mu W^+_\mu)] - A_\mu (W^+_\mu \partial_\nu W^-_ - \\
 & W^-_\mu \partial_\nu W^+_\mu) + A_\mu (W^+_\mu \partial_\nu W^-_ - W^-_\mu \partial_\nu W^+_\mu)] - \frac{1}{2}g^2 W^+_\mu W^-_ \mu W^+_\nu W^-_ \nu + \\
 & \frac{1}{2}g^2 W^+_\mu W^-_ \nu W^+_\nu W^-_ \nu + g^2 c_w^2 (Z^0_\mu W^+_\mu Z^0_\nu W^-_ \nu - Z^0_\mu Z^0_\nu W^+_\nu W^-_ \nu) + \\
 & g^2 s_w^2 (A_\mu W^+_\mu A_\nu W^-_ \nu - A_\mu A_\nu W^+_\nu W^-_ \nu) + g^2 s_w c_w [A_\mu Z^0_\nu (W^+_\mu W^-_ \nu - \\
 & W^+_\nu W^-_ \mu) - 2A_\mu Z^0_\mu W^+_\nu W^-_ \nu] - g_\alpha [H^3 + H \phi^0 \phi^0 + 2H \phi^+ \phi^-] - \\
 & \frac{1}{8}g^2 \alpha_h [H^4 + (\phi^0)^2 + 4(\phi^+ \phi^-)^2 + 4(\phi^0 \phi^+)^2 + 4H^2 \phi^+ \phi^- + 2(\phi^0)^2 H^2] - \\
 & g M W^+_\mu W^-_ \mu H - \frac{1}{2}g \frac{M}{c_w^2} Z^0_\mu Z^0_\nu H - \frac{1}{2}g [W^+_\mu (\phi^0 \partial_\mu \phi^- - \phi^- \partial_\mu \phi^0) - \\
 & W^-_\mu (\phi^0 \partial_\mu \phi^+ - \phi^- \partial_\mu \phi^0)] + \frac{1}{2}g [W^+_\mu (H \partial_\mu \phi^- - \phi^- \partial_\mu H) - W^-_\mu (H \partial_\mu \phi^+ - \\
 & \phi^+ \partial_\mu H)] + \frac{1}{2}g \frac{1}{c_w^2} (Z^0_\mu (H \partial_\mu \phi^0 - \phi^0 \partial_\mu H) - ig \frac{s_w^2}{c_w} M Z^0_\mu (W^+_\mu \phi^- - W^-_\mu \phi^+) + \\
 & ig s_w M A_\mu (W^+_\mu \phi^- - W^-_\mu \phi^+) - ig \frac{1-2c_w^2}{2c_w^2} Z^0_\mu (\phi^+ \partial_\mu \phi^- - \phi^- \partial_\mu \phi^+) + \\
 & ig s_w A_\mu (\phi^+ \partial_\mu \phi^- - \phi^- \partial_\mu \phi^+) - \frac{1}{4}g^2 W^+_\mu W^-_\mu [H^2 + (\phi^0)^2 + 2\phi^+ \phi^-] - \\
 & \frac{1}{4}g^2 \frac{1}{c_w^2} Z^0_\mu Z^0_\nu [H^2 + (\phi^0)^2 + 2(2s_w^2 - 1)^2 \phi^+ \phi^-] - \frac{1}{2}g^2 \frac{s_w^2}{c_w^2} Z^0_\mu \phi^0 (W^+_\mu \phi^- + \\
 & W^-_\mu \phi^+) - \frac{1}{2}ig^2 \frac{s_w^2}{c_w^2} Z^0_\mu H (W^+_\mu \phi^- - W^-_\mu \phi^+) + \frac{1}{2}g^2 s_w A_\mu \phi^0 (W^+_\mu \phi^- + \\
 & W^-_\mu \phi^+) + \frac{1}{2}ig^2 s_w A_\mu H (W^+_\mu \phi^- - W^-_\mu \phi^+) - g^2 \frac{s_w^2}{c_w^2} (2c_w^2 - 1) Z^0_\mu A_\mu \phi^+ \phi^- - \\
 & g^2 s_w^2 A_\mu A_\mu \phi^+ \phi^- - \bar{e}^\lambda (\gamma \partial + m_e^\lambda) e^\lambda - \bar{\nu}^\lambda \gamma^\mu \partial \bar{v}^\lambda - \bar{u}_j^\lambda (\gamma \partial + m_u^\lambda) u_j^\lambda - \\
 3 & d_j^\lambda (\gamma \partial + m_d^\lambda) d_j^\lambda + ig s_w A_\mu [-(\bar{e}^\lambda \gamma^\mu e^\lambda) + \frac{2}{3}(\bar{u}_j^\lambda \gamma^\mu u_j^\lambda) - \frac{1}{3}(\bar{d}_j^\lambda \gamma^\mu d_j^\lambda)] + \\
 & \frac{ig}{4c_w} Z^0_\mu [(\bar{\nu}^\lambda \gamma^\mu (1 + \gamma^5) \nu^\lambda) + (\bar{e}^\lambda \gamma^\mu (4s_w^2 - 1 - \gamma^5) e^\lambda) + (\bar{u}_j^\lambda \gamma^\mu (\frac{1}{2}s_w^2 - \\
 & 1 - \gamma^5) u_j^\lambda) + (d_j^\lambda \gamma^\mu (1 - \frac{3}{2}s_w^2 - \gamma^5) d_j^\lambda)] + \frac{ig}{\sqrt{2}} W^+_\mu [(\bar{\nu}^\lambda \gamma^\mu (1 + \gamma^5) e^\lambda) + \\
 & (\bar{u}_j^\lambda \gamma^\mu (1 + \gamma^5) C_{\lambda \kappa} d_j^\kappa)] + \frac{ig}{\sqrt{2}} W^-_\mu [(\bar{e}^\lambda \gamma^\mu (1 + \gamma^5) \nu^\lambda) + (\bar{d}_j^\lambda C_{\lambda \kappa}^\dagger \gamma^\mu (1 + \\
 & \gamma^5) u_j^\lambda)] + \frac{ig}{\sqrt{2}} \frac{m_e^2}{M} [-\phi^+ (\bar{\nu}^\lambda (1 - \gamma^5) e^\lambda) + \phi^- (\bar{e}^\lambda (1 + \gamma^5) \nu^\lambda)] - \\
 4 & \frac{g}{2} \frac{m_\lambda^2}{M} [H (\bar{e}^\lambda e^\lambda) + i \phi^0 (\bar{e}^\lambda \gamma^5 e^\lambda)] + \frac{ig}{2M \sqrt{2}} \phi^+ [-m_d^\lambda (\bar{u}_j^\lambda C_{\lambda \kappa} (1 - \gamma^5) d_j^\kappa) + \\
 & m_u^\lambda (\bar{u}_j^\lambda C_{\lambda \kappa} (1 + \gamma^5) d_j^\kappa) + \frac{ig}{2M \sqrt{2}} \phi^- [m_d^\lambda (\bar{d}_j^\lambda C_{\lambda \kappa}^\dagger (1 + \gamma^5) u_j^\kappa) - m_u^\kappa (\bar{d}_j^\lambda C_{\lambda \kappa}^\dagger (1 - \\
 & \gamma^5) u_j^\kappa]] - \frac{g}{2} \frac{m_\lambda^2}{M} H (\bar{u}_j^\lambda u_j^\lambda) - \frac{g}{2} \frac{m_\lambda^2}{M} H (\bar{d}_j^\lambda d_j^\lambda) + \frac{ig}{2} \frac{m_\lambda^2}{M} \phi^0 (\bar{u}_j^\lambda \gamma^5 u_j^\lambda) - \\
 & \frac{ig}{2} \frac{m_\lambda^2}{M} \phi^0 (\bar{d}_j^\lambda \gamma^5 d_j^\lambda) + \bar{X}^+(\partial^2 - M^2) X^+ + \bar{X}^-(\partial^2 - M^2) X^- + \bar{X}^0(\partial^2 - \\
 & \frac{M^2}{c_w^2}) X^0 + \bar{Y} \partial^2 Y + ig c_w W^+_\mu (\partial_\mu \bar{X}^0 X^- - \partial_\mu \bar{X}^0 X^+) + ig s_w W^+_\mu (\partial_\mu \bar{Y}^- Y - \\
 & \partial_\mu \bar{Y}^+ Y) + ig c_w W^-_\mu (\partial_\mu \bar{X}^- X^0 - \partial_\mu \bar{X}^0 X^-) + ig s_w W^-_\mu (\partial_\mu \bar{Y}^+ Y - \\
 & \partial_\mu \bar{Y}^- Y) + ig c_w Z^0_\mu (\partial_\mu \bar{X}^+ X^+ - \partial_\mu \bar{X}^- X^-) + ig s_w A_\mu (\partial_\mu \bar{X}^+ X^+ - \\
 & \partial_\mu \bar{X}^- X^-) - \frac{1}{2}g M [\bar{X}^+ X^+ H + \bar{X}^- X^- H + \frac{1}{c_w^2} \bar{X}^0 X^0 H] + \\
 & \frac{1-2c_w^2}{2c_w^2} ig M [\bar{X}^+ X^0 \phi^- - \bar{X}^- X^0 \phi^+] + \frac{1}{2c_w^2} ig M [\bar{X}^0 X^- \phi^+ - \bar{X}^0 X^+ \phi^-] + \\
 & ig M s_w [\bar{X}^0 X^- \phi^+ - \bar{X}^0 X^+ \phi^-] + \frac{1}{2}ig M [\bar{X}^+ X^+ \phi^0 - \bar{X}^- X^- \phi^0]
 \end{aligned}$$

Reminder

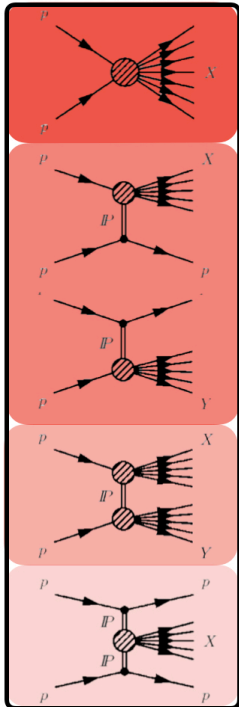
Standard Model

Lagrangian of the SM

- 1 QCD sector
- 2 EW sector for boson-only interactions
- 3 EW sector for boson-fermions interactions
- 4 (Higgs ghosts)
- 5 (Faddeev-Popov ghosts)

At LHC

Since we essentially collide protons, which are composite particles made of quarks and gluons strongly interacting, 99% of the interactions can be explained with QCD only!



Reminder

Phenomenology

Total cross section at LHC at 13 TeV

type	total cross section
total	~ 100 mb
elastic	~ 24 mb
inelastic	~ 76 mb
\rightarrow single-diffractive	~ 15 mb
\rightarrow double-diffractive	~ 10 mb
\rightarrow central-diffractive	~ 1 mb
\rightarrow non-diffractive	~ 50 mb

PYTHIA 8 prediction at $\sqrt{s} = 13$ TeV

Introduction

Reminder

Goal

Motivation

Experimental data

Experimental analysis

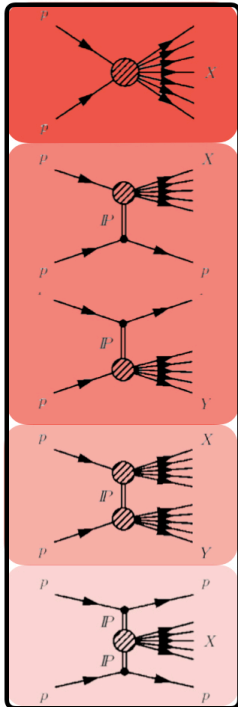
Results

Interpretation

Methods

Summary & Conclusions

Back-up



Reminder

Phenomenology

Total cross section at LHC at 13 TeV

type	total cross section
total	~ 100 mb
elastic	~ 24 mb
inelastic	~ 76 mb
\rightarrow single-diffractive	~ 15 mb
\rightarrow double-diffractive	~ 10 mb
\rightarrow central-diffractive	~ 1 mb
\rightarrow non-diffractive	~ 50 mb

PYTHIA 8 prediction at $\sqrt{s} = 13$ TeV

Type of collisions of interest for this measurement

Inelastic non-diffractive scattering with large momentum transfer
in proton-proton collisions

$$\sigma(p_T > 15 \text{ GeV}) \approx 1 - 2 \text{ mb only}$$

and this is still a huge background for most analyses...

Introduction

Reminder

Goal

Motivation

Experimental data

Experimental analysis

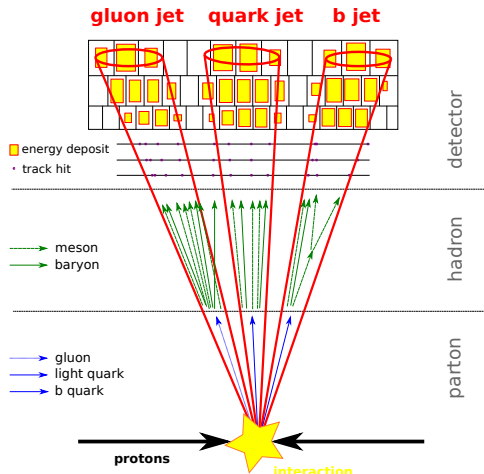
Results

Interpretation

Methods

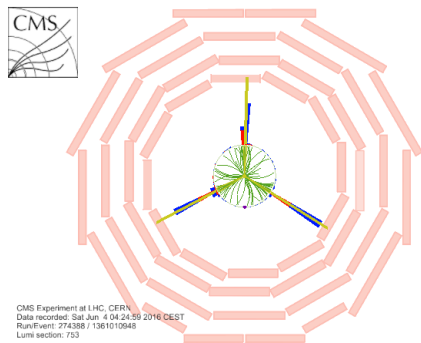
Summary & Conclusions

Back-up



Reminder

Jets



Jets

- Collection of particles in a region of the detector.
- Result of strong interactions (hadronisation process).
- Directly probing highest-energy part of the process.

Introduction

Reminder

Goal

Motivation

Experimental data

Experimental analysis

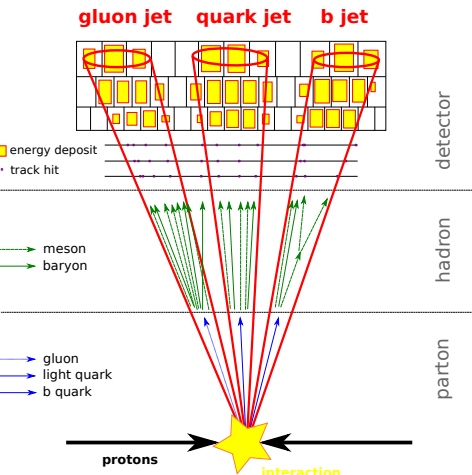
Results

Interpretation

Methods

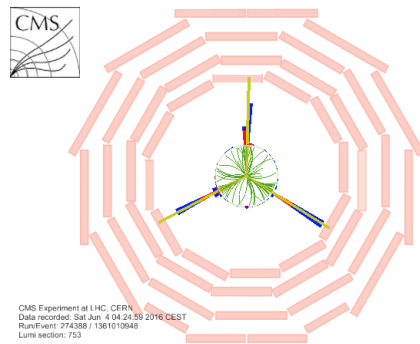
Summary & Conclusions

Back-up



Reminder

Jets



Jets

- Collection of particles in a region of the detector.
- Result of strong interactions (hadronisation process).
- Directly probing highest-energy part of the process.

Clustering algorithms [1, 2]

- Cambridge-Aachen
- k_T
- $\text{anti-}k_T$

→ free parameter R

Introduction

Reminder

Goal

Motivation

Experimental

data

Experimental
analysis

Results

Interpreta-
tion

Methods

Summary &
Conclusions

Back-up

Goal

Inclusive jet production

Measure the double-differential cross section

$$\frac{d^2\sigma}{dp_T dy} = \frac{1}{\mathcal{L}} \frac{N_{\text{jets}}^{\text{eff}}}{\Delta p_T \Delta y} \quad (1)$$

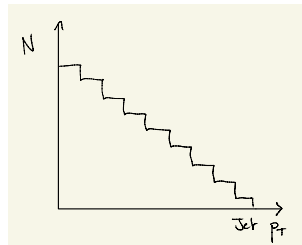
with recorded at the CMS experiment in pp collisions during the year 2016.

p_T transverse momentum;

y rapidity $\equiv \log \frac{E+p_z}{E-p_z} \sim -\log \tan \frac{\theta}{2}$;

$N_{\text{jets}}^{\text{eff}}$ effective number of jets after all corrections from experimental effects;

\mathcal{L} integrated luminosity.



Introduction

Reminder

Goal

Motivation

Experimental

data

Experimental
analysis

Results

Interpretation

Methods

Summary &
Conclusions

Back-up

Goal

Inclusive jet production

Measure the double-differential cross section

$$\frac{d^2\sigma}{dp_T dy} = \frac{1}{\mathcal{L}} \frac{N_{\text{jets}}^{\text{eff}}}{\Delta p_T \Delta y} \quad (1)$$

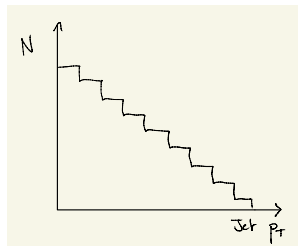
with recorded at the CMS experiment in pp collisions during the year 2016.

p_T transverse momentum;

y rapidity $\equiv \log \frac{E+p_z}{E-p_z} \sim -\log \tan \frac{\theta}{2}$;

$N_{\text{jets}}^{\text{eff}}$ effective number of jets after all corrections from experimental effects;

\mathcal{L} integrated luminosity.



Challenge

Achieve **percent-level** precision of a **steeply falling** spectrum over several orders of magnitude and demonstrate usability of the data by global PDF collaborations and for searches!



Introduction

Reminder

Goal

Motivation

Experimental

data

Experimental
analysis

Results

Interpreta-
tion

Methods

Summary &
Conclusions

Back-up

Motivation

Factorisation [3]

$$\underbrace{\sigma_{pp \rightarrow \text{jet}+X}}_{\text{experimental data}} = \sum_{ij \in gq\bar{q}} \overbrace{f_i(x_i, \mu_F^2) \otimes f_j(x_j, \mu_F^2)}^{\text{PDFs}} \\ \otimes \hat{\sigma}_{ij \rightarrow \text{jet}+X} \left(x_i, x_j, \frac{Q^2}{\mu_F^2}, \frac{Q^2}{\mu_R^2}, \alpha_S(\mu_R^2) \right) \underbrace{\quad}_{\text{SM or ...}}$$

State-of-the art
calculations

NNLO or NLO+NLL FO
predictions.



Introduction
Reminder
Goal
Motivation
Experimental data

Experimental analysis

Results

Interpretation

Methods

Summary & Conclusions

Back-up



Factorisation [3]

$$\underbrace{\sigma_{pp \rightarrow \text{jet}+X}}_{\text{experimental data}} = \sum_{ij \in gq\bar{q}} \overbrace{f_i(x_i, \mu_F^2) \otimes f_j(x_j, \mu_F^2)}^{\text{PDFs}} \\ \otimes \hat{\sigma}_{ij \rightarrow \text{jet}+X} \left(x_i, x_j, \frac{Q^2}{\mu_F^2}, \frac{Q^2}{\mu_R^2}, \alpha_S(\mu_R^2) \right) \\ \text{SM or SMEFT}$$

Motivation

State-of-the art calculations

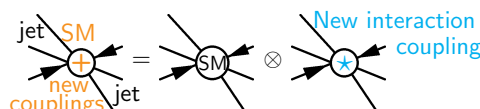
NNLO or NLO+NLL FO predictions.

Contact Interactions (CIs)

$$\mathcal{L}_{\text{SMEFT}} = \mathcal{L}_{\text{SM}} + \frac{4\pi}{2\Lambda^2} \sum_n c_n O_n$$

CI model	c_1	c_3	c_5
Purely left-handed	free	0	0
Vector-like	free	$2c_1$	c_1
Axial-vector-like	free	$-2c_1$	c_1

NB: colour-singlet model



Introduction

Reminder

Goal

Motivation

Experimental data

Experimental analysis

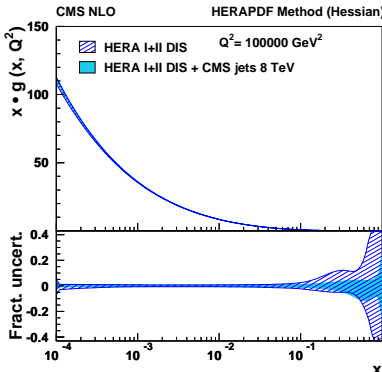
Results

Interpretation

Methods

Summary & Conclusions

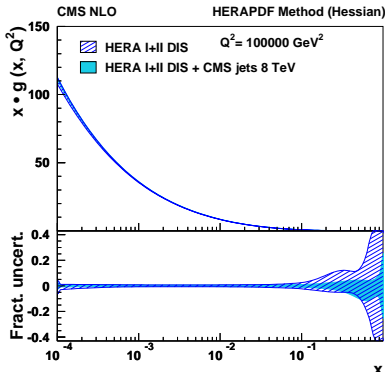
Back-up



Motivation

Former inclusive jet measurements at LHC

\sqrt{s}	ATLAS	CMS
2.76 TeV	0.0002 fb^{-1} [4]	0.0054 fb^{-1} [5]
7 TeV	4.5 fb^{-1} [6]	5.0 fb^{-1} [7, 8]
8 TeV	20 fb^{-1} [9]	20 fb^{-1} [10]
13 TeV	3.2 fb^{-1} [11]	0.071 fb^{-1} [12]



Motivation

Former inclusive jet measurements at LHC

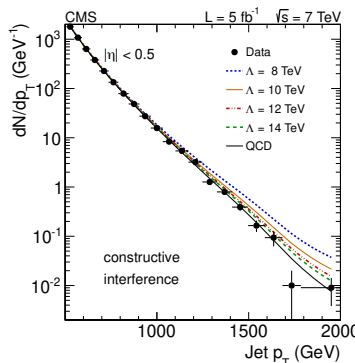
\sqrt{s}	ATLAS	CMS
2.76 TeV	0.0002 fb ⁻¹ [4]	0.0054 fb ⁻¹ [5]
7 TeV	4.5 fb ⁻¹ [6]	5.0 fb ⁻¹ [7, 8]
8 TeV	20 fb ⁻¹ [9]	20 fb ⁻¹ [10]
13 TeV	3.2 fb ⁻¹ [11]	0.071 fb ⁻¹ [12]

Searches for Cls at CMS [13, 14]

- Fold SMEFT predictions with existing PDF.
 - Constrain CIs (Wilson coefficient c_1).

Question

But **what if** the Cls have already been absorbed in the PDF?



Introduction

Reminder

Goal

Motivation

Experimental data

Experimental analysis

Results

Interpretation

Methods

Summary & Conclusions

Back-up



Motivation

Perform **simultaneous fit** of PDFs, α_S , m_t , and **Wilson coefficient** c_1 !

Phase space [15]

- $p_T > 97 \text{ GeV}$
- $|y| < 2.0$

Measurement

- High-PU 2016 data using anti- k_T jet clustering algorithm.
- Systematic effects corrected via 2D sample unfolding.

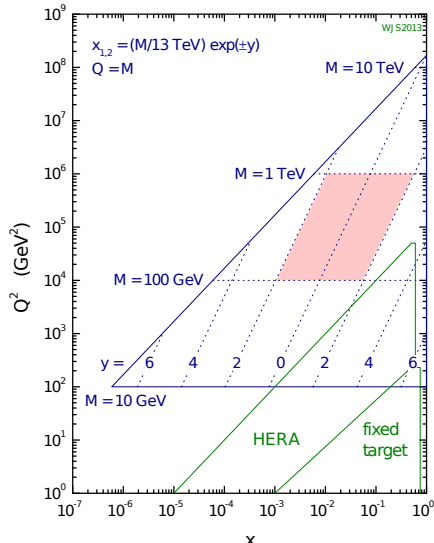
QCD interpretation

Using xFitter [16, 17]:

- HERA DIS data [18],
- CMS $t\bar{t}$ 3D cross section at 13 TeV [19],
- CMS inclusive jet 2D cross section at 13 TeV [20].

Experimental data

13 TeV LHC parton kinematics



Experimental analysis

Strategy

Counting

Jet energy calibration

Pile-up corrections

Unfolding

Introduction

Experimental analysis

Strategy

Counting

Jet energy calibration

Pile-up corrections

Unfolding

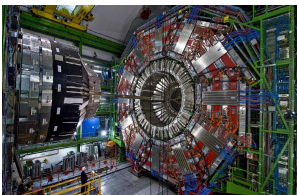
Results

Interpretation

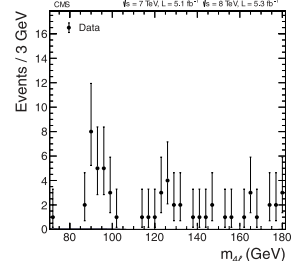
Methods

Summary & Conclusions

Back-up



Strategy



Introduction

Experimental analysis

Strategy

Counting

Jet energy calibration

Pile-up corrections

Unfolding

Results

Interpretation

Methods

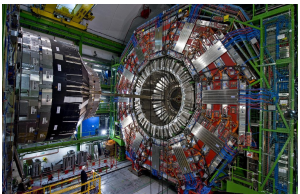
Summary & Conclusions

Back-up

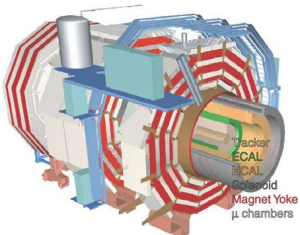
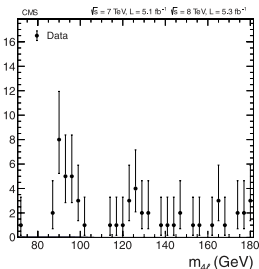
UH



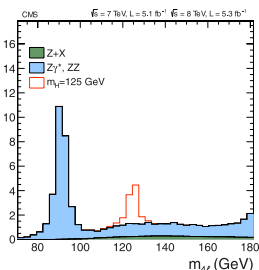
Strategy



Events / 3 GeV



Events / 3 GeV



Introduction

Experimental analysis

Strategy

Counting

Jet energy calibration

Pile-up corrections

Unfolding

Results

Interpretation

Methods

Summary & Conclusions

Back-up

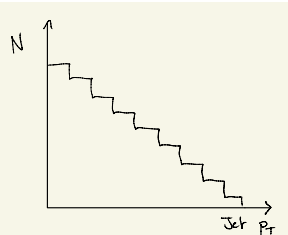
Strategy

Data

- $\mathcal{L}_{\text{int}} = 36.3(33.5) \text{ fb}^{-1}$.
- Jet clustering with AK4 (AK7).

Corrections

- Counting
- Jet energy corrections
- Pile-up corrections
- Unfolding with simulated data



Strategy

Introduction

Experimental analysis

Strategy

Counting

Jet energy calibration

Pile-up corrections

Unfolding

Results

Interpretation

Methods

Summary & Conclusions

Back-up

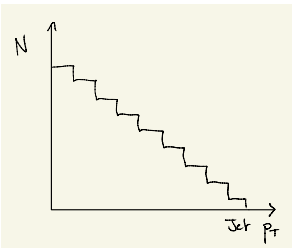


Data

- $\mathcal{L}_{\text{int}} = 36.3(33.5) \text{ fb}^{-1}$.
- Jet clustering with AK4 (AK7).

Corrections

- Counting
- Jet energy corrections
- Pile-up corrections
- Unfolding with simulated data



generator	PDF	matrix element	tune
PYTHIA 8 (230) [21]	NNPDF 2.3 [22]	LO $2 \rightarrow 2$	CUETP8M1 [23]
MADGRAPH_MC@NLO (2.4.3) [24, 25]	NNPDF 2.3 [22]	LO $2 \rightarrow 2, 3, 4$	CUETP8M1 [23]
HERWIG++ (2.7.1) [26]	CTEQ6L1 [27]	LO $2 \rightarrow 2$	CUETHppS1 [23]

Introduction

Experimental analysis

Strategy

Counting

Jet energy calibration

Pile-up corrections

Unfolding

Results

Interpretation

Methods

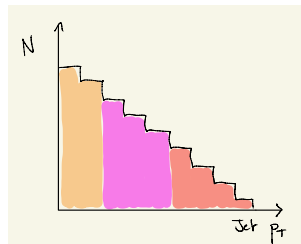
Summary & Conclusions

Back-up

Triggers

- Bunches cross every 25 ns at CMS
 - production rate is several order of magnitudes too large to record all jets.
 - Record jets with different rates according to their energy
 - multiply by prescale factor in counting of jets for calculation of cross section.
- **Fast reconstruction** algorithm (L1 & HLT) are used to identify on the fly the presence of jets, then roughly **estimate their energy**.

Counting



$p_T^{\text{HLT}} (\text{GeV})$	40	60	80	140	200	260	320	400	450
$p_T^{\text{PF}} (\text{GeV})$	74–97	97–133	133–196	196–272	272–362	362–430	430–548	548–592	>592
$\mathcal{L} (\text{pb}^{-1})$	0.267	0.726	2.76	24.2	103	594	1770	5190	36300



Introduction

Experimental analysis

Strategy

Counting

Jet energy calibration

Pile-up corrections

Unfolding

Results

Interpretation

Methods

Summary & Conclusions

Back-up

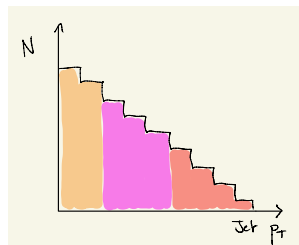
UH



Triggers

- Bunches cross every 25 ns at CMS
 - production rate is several order of magnitudes too large to record all jets.
 - Record jets with different rates according to their energy
 - multiply by prescale factor in counting of jets for calculation of cross section.
- **Fast reconstruction** algorithm (L1 & HLT) are used to identify on the fly the presence of jets, then roughly **estimate their energy**.

Counting



$p_T^{\text{HLT}} (\text{GeV})$	40	60	80	140	200	260	320	400	450
$p_T^{\text{PF}} (\text{GeV})$	74–97	97–133	133–196	196–272	272–362	362–430	430–548	548–592	>592
$\mathcal{L} (\text{pb}^{-1})$	0.267	0.726	2.76	24.2	103	594	1770	5190	36300

Uncertainties

- Statistical correlations (multi-count observable)
- Luminosity \mathcal{L} (correlated 1.2%)
- Trigger uncertainty (uncorrelated 0.2%)
- Inefficiencies (e.g. ECAL prefireing)

Introduction

Experimental analysis

Strategy

Counting

Jet energy calibration

Pile-up corrections

Unfolding

Results

Interpretation

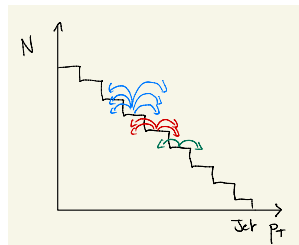
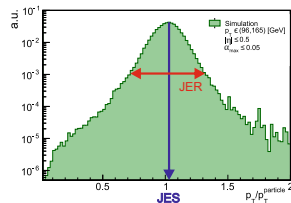
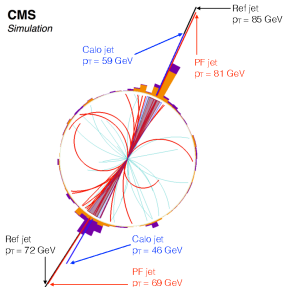
Methods

Summary & Conclusions

Back-up



Jet energy calibration



Corrections

Scale $\langle p_T^{\text{gen}} \rangle \approx \langle p_T^{\text{rec}} \rangle$ both in real and simulated data

Resolution smearing rate from true level to detector level should be the same in simulated data as in real data

→ Many sources of uncertainties related to various effects (not discussed in this presentation).

Introduction

Experimental analysis

Strategy

Counting

Jet energy calibration

Pile-up corrections

Unfolding

Results

Interpretation

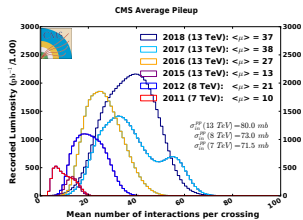
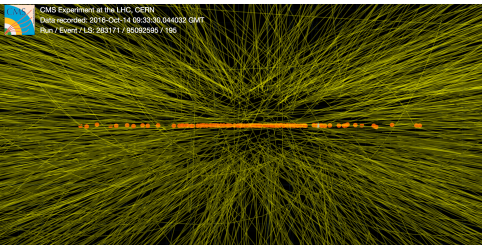
Methods

Summary & Conclusions

Back-up



Pile-up corrections



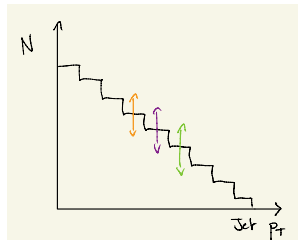
Reminder

Several pp collisions at each bunch crossing:

Pros higher chances for rare events (high p_T).

Cons

- distinctions among collisions more difficult (multiplicity);
- additional contribution to jets (offset).



PU profile correction

Correct the profile of simulated data to profile in real data by event reweighting
 → additional uncertainty from minimum-bias cross section.

A black and white astronomical photograph of a celestial object. The central feature is a bright, roughly circular nebula with a visible internal structure, characteristic of a planetary nebula or a star-forming region. It is surrounded by a faint, diffuse glow. Several smaller, distinct stars of varying brightness are scattered across the dark background sky.

IC-1296





Introduction

Experimental analysis

Strategy

Counting

Jet energy calibration

Pile-up corrections

Unfolding

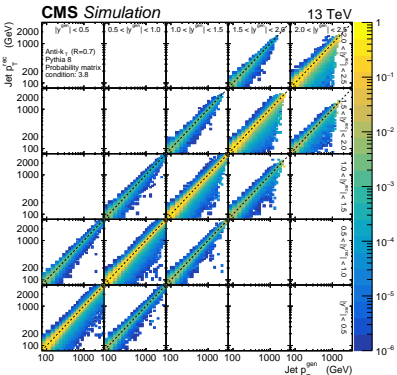
Results

Interpretation

Methods

Summary & Conclusions

Back-up



Unfolding

Matrix inversion

For binned data:

$$\mathbf{Ax} + \mathbf{b} = \mathbf{y} \quad (2)$$

- x** data distribution at particle level
- y** data distribution at detector level
- b** background spectrum at detector level
- A** probability matrix (figure)

→ instable...

Least-square minimisation [28, 29]

with $\#\text{detector-level bins} = 2 \times \#\text{particle-level bins}$

(but no Tikhonov regularisation)

$$\chi^2 = \min_{\mathbf{x}} [(\mathbf{Ax} + \mathbf{b} - \mathbf{y})^T \mathbf{V}^{-1} (\mathbf{Ax} + \mathbf{b} - \mathbf{y})] \quad (3)$$

V covariance matrix accounting for partial correlations



Introduction

Experimental analysis

Strategy

Counting

Jet energy calibration

Pile-up corrections

Unfolding

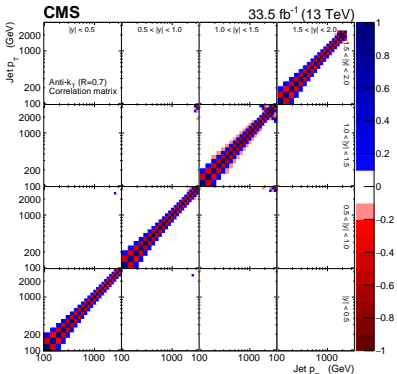
Results

Interpretation

Methods

Summary & Conclusions

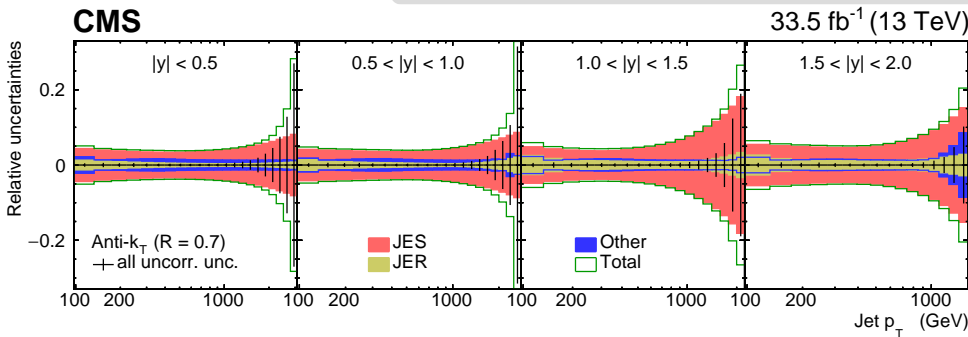
Back-up



Unfolding

Uncertainties

- The limited statistics of the simulated data contributes as an extra uncertainty.
- Additional uncertainties on migrations across the edges of the phase space are included (but very small).
- All other uncertainties are inferred to particle-level by applying the variations either in the input data or in the probability matrix (and smoothed).



Results

Overview

Event display

Comparison

Introduction

Experimental analysis

Results

Overview

Event display

Comparison

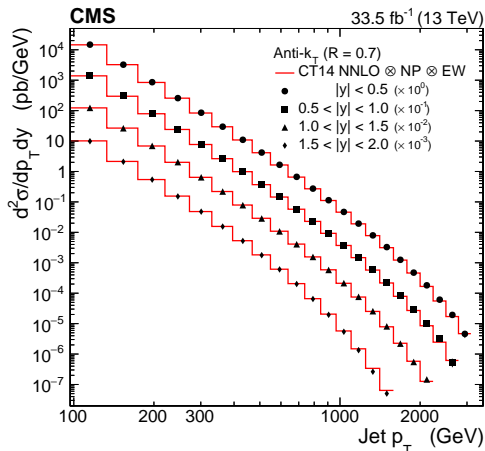
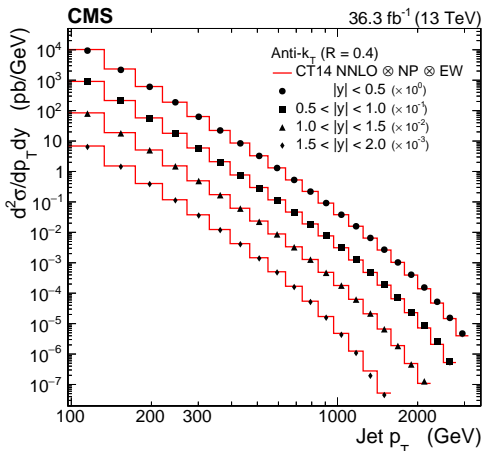
Interpretation

Methods

Summary & Conclusions

Back-up

Overview



Introduction

Experimental analysis

Results

Overview

Event display

Comparison

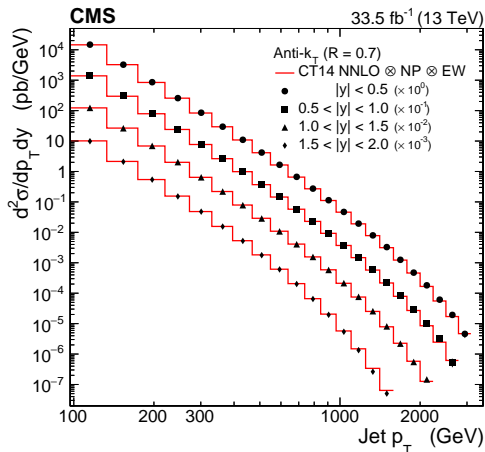
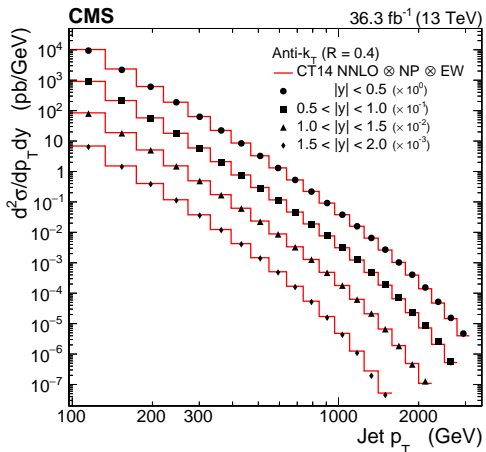
Interpretation

Methods

Summary & Conclusions

Back-up

Overview



Remark

- Looking for percent-level precision in steeply falling spectrum...
- But logarithmic scale can hide monsters!

→ Apply tests of smoothness [30] (more at the symposium!).

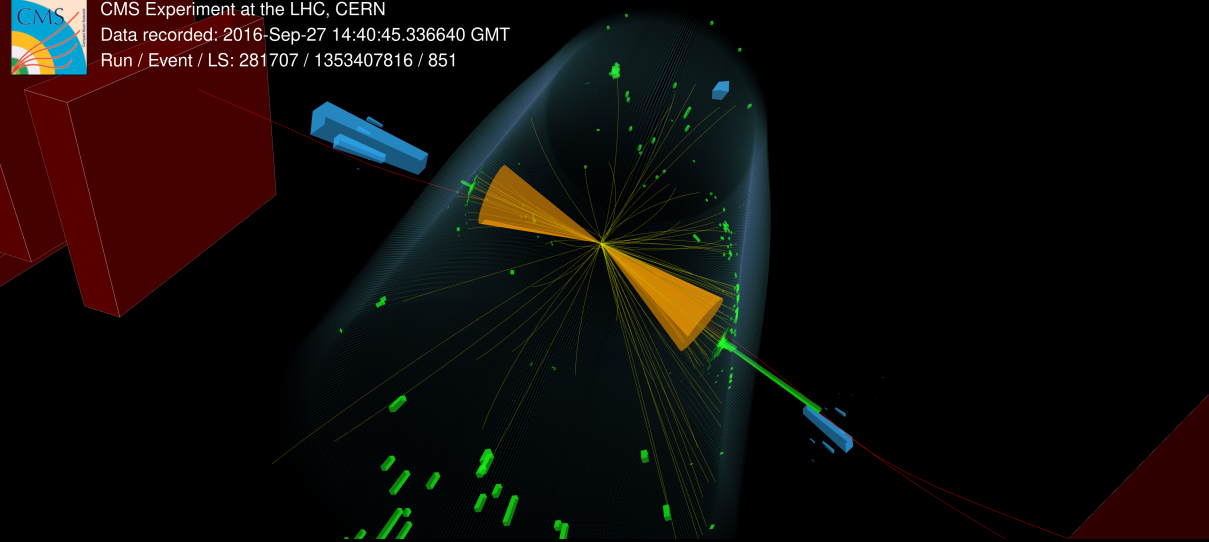




CMS Experiment at the LHC, CERN

Data recorded: 2016-Sep-27 14:40:45.336640 GMT

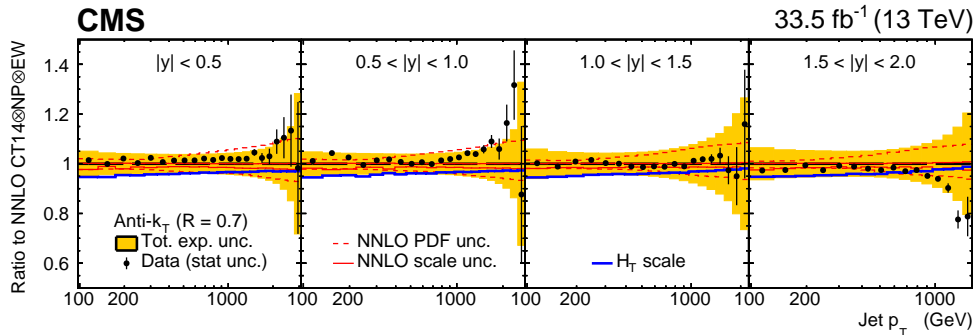
Run / Event / LS: 281707 / 1353407816 / 851



Ref. [31]

Comparison

Introduction
Experimental analysis
Results
Overview
Event display
Comparison
Interpretation
Methods
Summary & Conclusions
Back-up



Inclusive jet cross section (SMP-20-011 [20])

- Comparison to various global PDF [18, 32, 33, 34, 35] sets with NLO+NLL [36].



Introduction

Experimental analysis

Results

Overview

Event display

Comparison

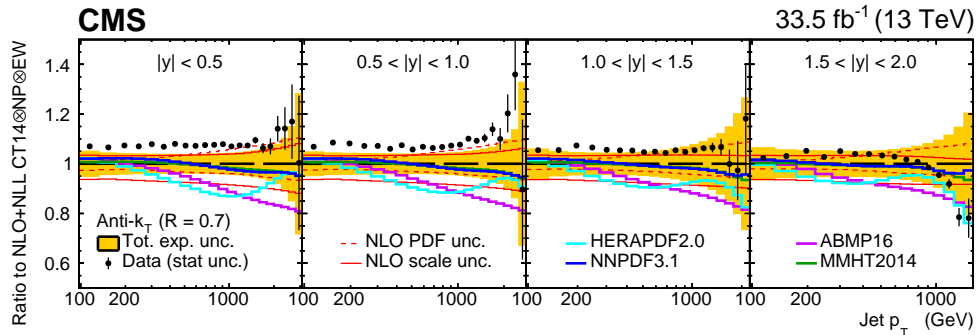
Interpretation

Methods

Summary & Conclusions

Back-up

Comparison



Inclusive jet cross section (SMP-20-011 [20])

- Comparison to various global PDF [18, 32, 33, 34, 35] sets with NLO+NLL [36].
- Comparison to NNLO obtained with NNLOJET [37, 38, 39].



Interpretation

Strategy

SM fits

SMEFT fits

Introduction

Experimental analysis

Results

Interpretation

Strategy

SM fits

SMEFT fits

Methods

Summary & Conclusions

Back-up

Strategy

Impact on PDFs

Profiling investigate reduction of uncertainties on existing PDF sets(not discussed here).

Full fits take a parameterisation of PDF sets and combine data with other data sets.

→ Here, we perform **full fits** with FO predictions at NNLO with present data combined to HERA DIS data and to a former CMS $t\bar{t}$ measurement at 13 TeV, and extract $\alpha_S(M_Z)$ and m_t in addition to PDFs.

Search for CIs

Using the same data sets, we perform fits at NLO+NLL with a fit of the c_1 Wilson coefficient in addition.



Introduction

Experimental analysis

Results

Interpretation

Strategy

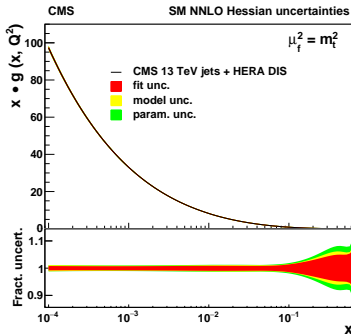
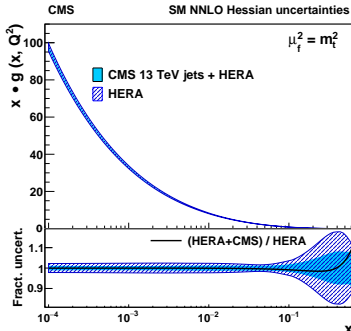
SM fits

SMEFT fits

Methods

Summary & Conclusions

Back-up



SM fits

Parameterisation

$$xg(x) = A_g x^{B_g} (1-x)^{C_g} (1+E_g x^2)$$

$$xu_v(x) = A_{u_v} x^{B_{u_v}} (1-x)^{C_{u_v}} (1+D_{u_v} x)$$

$$xd_v(x) = A_{d_v} x^{B_{d_v}} (1-x)^{C_{d_v}}$$

$$x\bar{U}(x) = A_{\bar{U}} x^{B_{\bar{U}}} (1-x)^{C_{\bar{U}}}$$

$$x\bar{D}(x) = A_{\bar{D}} x^{B_{\bar{D}}} (1-x)^{C_{\bar{D}}}$$

Results

- Strong reduction of the gluon PDF uncertainty.

Introduction

Experimental analysis

Results

Interpretation

Strategy

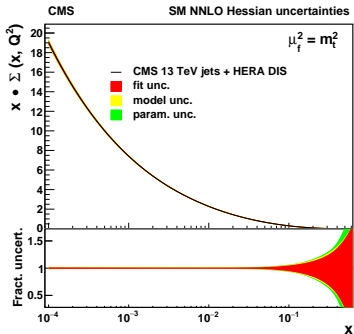
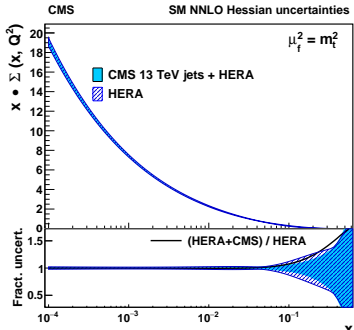
SM fits

SMEFT fits

Methods

Summary & Conclusions

Back-up



SM fits

Parameterisation

$$xg(x) = A_g x^{B_g} (1-x)^{C_g} (1+E_g x^2)$$

$$xu_v(x) = A_{u_v} x^{B_{u_v}} (1-x)^{C_{u_v}} (1+D_{u_v} x)$$

$$xd_v(x) = A_{d_v} x^{B_{d_v}} (1-x)^{C_{d_v}}$$

$$x\bar{U}(x) = A_{\bar{U}} x^{B_{\bar{U}}} (1-x)^{C_{\bar{U}}}$$

$$x\bar{D}(x) = A_{\bar{D}} x^{B_{\bar{D}}} (1-x)^{C_{\bar{D}}}$$

Results

- Strong reduction of the gluon PDF uncertainty.
- Strong reduction of α_S uncertainty.

SM parameters

$$\alpha_S = 0.1188 \pm 0.0017(\text{fit}) \pm 0.0022(\text{model and param.})$$

$$m_t^{\text{pole}} = 170.4 \pm 0.6(\text{fit}) \pm 0.1(\text{model and param.})$$

SM fits

Introduction

Experimental analysis

Results

Interpretation

Strategy

SM fits

SMEFT fits

Methods

Summary & Conclusions

Back-up

Data sets		HERA-only Partial χ^2/N_{dp}	HERA+CMS Partial χ^2/N_{dp}
HERA I+II neutral current	$e^+ p, E_p = 920 \text{ GeV}$	378/332	375/332
HERA I+II neutral current	$e^+ p, E_p = 820 \text{ GeV}$	60/63	60/63
HERA I+II neutral current	$e^+ p, E_p = 575 \text{ GeV}$	201/234	201/234
HERA I+II neutral current	$e^+ p, E_p = 460 \text{ GeV}$	208/187	209/187
HERA I+II neutral current	$e^- p, E_p = 920 \text{ GeV}$	223/159	227/159
HERA I+II charged current	$e^+ p, E_p = 920 \text{ GeV}$	46/39	46/39
HERA I+II charged current	$e^- p, E_p = 920 \text{ GeV}$	55/42	56/42
CMS inclusive jets 13 TeV	$0.0 < y < 0.5$	—	13/22
	$0.5 < y < 1.0$	—	31/21
	$1.0 < y < 1.5$	—	18/19
	$1.5 < y < 2.0$	—	14/16
Correlated χ^2		66	83
Global χ^2/N_{dof}		1231/1043	1321/1118



Introduction

Experimental analysis

Results

Interpretation

Strategy

SM fits

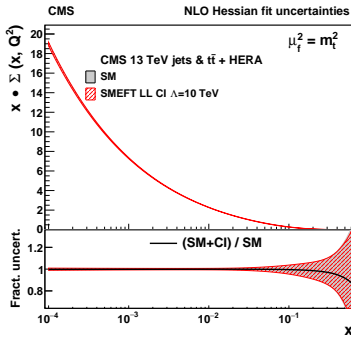
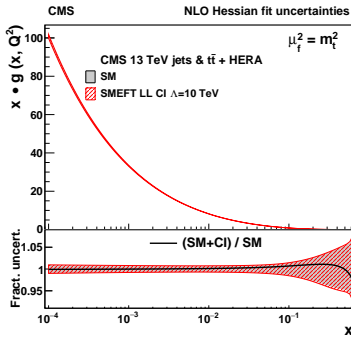
SMEFT fits

Methods

Summary & Conclusions

Back-up

UH



SMEFT fits

Parameterisation

$$xg(x) = A_g x^{B_g} (1-x)^{C_g} (1+E_g x^2)$$

$$xu_v(x) = A_{u_v} x^{B_{u_v}} (1-x)^{C_{u_v}} (1+D_{u_v} x + E_{u_v} x^2)$$

$$xd_v(x) = A_{d_v} x^{B_{d_v}} (1-x)^{C_{d_v}} (1+D_{d_v} x)$$

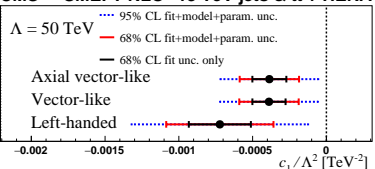
$$x\bar{U}(x) = A_{\bar{U}} x^{B_{\bar{U}}} (1-x)^{C_{\bar{U}}}$$

$$x\bar{D}(x) = A_{\bar{D}} x^{B_{\bar{D}}} (1-x)^{C_{\bar{D}}}$$

Results

SMEFT fits lead to results compatible w. SM.

CMS SMEFT NLO 13 TeV jets & $t\bar{t}$ + HERA



Methods

DAS

CDCS



Das Analysis-System (<https://gitlab.cern.ch/DasAnalysisSystem>)

- Recompile the code while some jobs were running
- Take a whole week to produce n -tuples
- Lost in one's own code
- Lost with large amount of flags
- Wait 24h to check the implementation of a new feature
- Compilation takes a few minutes
- Normalisation failing after a looong event loop
- Analysis code is 5000 lines long
- Synchronisation with other analyses too difficult
- Not enough storage for different versions of the n -tuples
- Missing documentation
- Code gets broken after an unfortunate push from a colleague
- One event in the middle of the n -tuple is corrupted
- etc.

→ Design of analysis software optimises debugging time.

Physics analyses

- Many **similar analyses** sensitive to the same physics.
- Non-replicable results & inconsistent **analysis strategies**.
- Short-term development & no view **beyond ongoing analyses**.

→ Trying to improve re-usability of implementation!

Introduction

Experimental analysis

Results

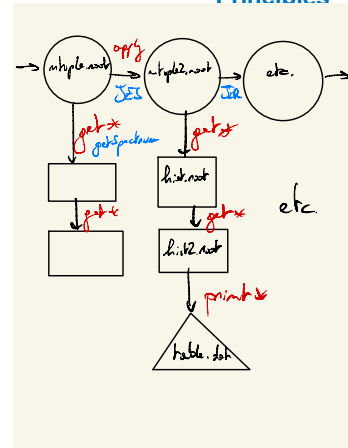
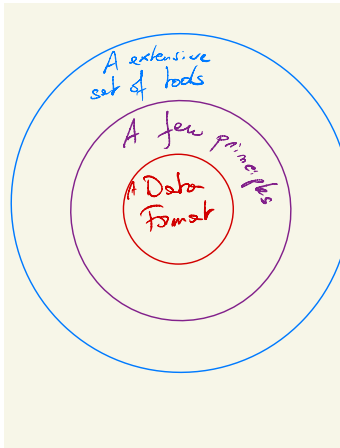
Interpretation

Methods
DAS
CDCSSummary &
Conclusions

Back-up

DAS

Principles



The three principles

- ① A data format
- ② Good programming conventions
- ③ Series of existing tools

→ *essential*

→ *exceptions should be allowed*

→ *up to the user*

Introduction

Experimental analysis

Results

Interpretation

Methods

DAS
CDCSSummary &
Conclusions

Back-up

UH



Smoothness

- Test quality of statistical description of differential distributions.
- Serious impact on QCD fits.

→ paper in preparation & presentation at symposium!

Refinement

- By-pass time-expensive simulation of the detector with fast-simulation and machine-learning techniques.
- Allow large statistical samples to better describe uncovered systematic effects (e.g. model uncertainties).

→ poster by Shruthi JANARDHAN at symposium!

Summary & Conclusions



Summary & Conclusions

- The CMS Collaboration has produced a measurement of **inclusive jet** production in pp collisions at 13 TeV:
 - ▶ the **experimental analysis** includes corrections to the jet count, the jet energy, and the pile-up; all effects are corrected via the procedure of unfolding;
 - ▶ data are compared to **FO predictions** at NLO+NLL and NNLO.
- A **novel QCD interpretation** including profiling studies and unbiased search for CI has been presented:
 - ▶ one of the **most precise** measurements of the strong coupling;
 - ▶ **no evidence for CI** has been found.
- Several advanced developments have started with this analysis and are continuing:
 - ▶ a framework optimised for debugging and replicability;
 - ▶ specific methods, such as tests of smoothness and refinement;
 - ▶ ...

→ *The paper has been recently published in JHEP!*

Thank you for your attention!

Back-up

[Acronyms](#)[References](#)[Visiting card](#)

AK4 anti k_T algorithm ($R = 0.4$). 20, 21

AK7 anti k_T algorithm ($R = 0.7$). 20, 21

CI Contact Interaction. 12–15, 37, 47

CMS Compact Muon Solenoid. 3, 10, 11, 14–16, 22, 23, 37, 47

DIS Deeply Inelastic Scattering. 16, 37

ECAL Electromagnetic CALorimeter. 22, 23

EW Electroweak. 4, 5

FO fixed order. 12, 13, 37, 47

HERA *Hadron-Elektron-RingAnlage*. 16, 37

HLT High-Level Trigger. 22, 23

Acronyms I

L1 Level 1. 22, 23

LHC Large Hadron Collider. 3–7, 14, 15

NLL Next to Leading Logarithm. 12, 13, 34, 35, 37, 47

NLO Next to Leading Order. 12, 13, 34, 35, 37, 47

NNLO Next to Next to Leading Order. 12, 13, 34, 35, 37, 47

PDF Parton Distribution Function. 10–16, 34, 35, 37–39

PU Pile-Up. 16, 25

QCD Quantum Chromodynamics. 4, 5, 16, 45, 47

SM Standard Model. 4, 5, 12, 13, 38, 39, 41

SMEFT Standard Model Effective Field Theory. 12–15, 41





References I

-  Matteo Cacciari, Gavin P. Salam, and Gregory Soyez. "The anti- k_t jet clustering algorithm". In: **JHEP** 04 (2008), p. 063. doi: 10.1088/1126-6708/2008/04/063. arXiv: 0802.1189 [hep-ph].
-  Matteo Cacciari, Gavin P. Salam, and Gregory Soyez. "FastJet User Manual". In: **Eur. Phys. J. C** 72 (2012), p. 1896. doi: 10.1140/epjc/s10052-012-1896-2. arXiv: 1111.6097 [hep-ph].
-  John C. Collins, Davison E. Soper, and George F. Sterman. "Factorization of Hard Processes in QCD". In: **Adv. Ser. Direct. High Energy Phys.** 5 (1989), pp. 1–91. doi: 10.1142/9789814503266_0001. arXiv: hep-ph/0409313 [hep-ph].
-  Georges Aad et al. "Measurement of the inclusive jet cross section in pp collisions at $\sqrt{s} = 2.76$ TeV and comparison to the inclusive jet cross section at $\sqrt{s} = 7$ TeV using the ATLAS detector". In: **Eur. Phys. J. C** 73 (2013), p. 2509. doi: 10.1140/epjc/s10052-013-2509-4. arXiv: 1304.4739 [hep-ex].
-  Vardan Khachatryan et al. "Measurement of the inclusive jet cross section in pp collisions at $\sqrt{s} = 2.76$ TeV". In: **Eur. Phys. J. C** 76 (2016), p. 265. doi: 10.1140/epjc/s10052-016-4083-z. arXiv: 1512.06212 [hep-ex].

References II

-  **Georges Aad et al.** "Measurement of the inclusive jet cross-section in proton-proton collisions at $\sqrt{s} = 7$ TeV using 4.5 fb^{-1} of data with the ATLAS detector". In: **JHEP** 02 (2015). [Erratum: **JHEP** 09, 141 (2015)], p. 153. DOI: [10.1007/JHEP02\(2015\)153](https://doi.org/10.1007/JHEP02(2015)153). arXiv: [1410.8857](https://arxiv.org/abs/1410.8857) [hep-ex].
-  **Serguei Chatrchyan et al.** "Measurements of Differential Jet Cross Sections in Proton-Proton Collisions at $\sqrt{s} = 7$ TeV with the CMS Detector". In: **Phys. Rev. D** 87 (2013). [Erratum: **JHEP** 09, 141 (2015)], p. 112002. DOI: [10.1103/PhysRevD.87.112002](https://doi.org/10.1103/PhysRevD.87.112002). arXiv: [1212.6660](https://arxiv.org/abs/1212.6660) [hep-ex].
-  **Serguei Chatrchyan et al.** "Measurement of the Ratio of Inclusive Jet Cross Sections using the Anti- k_T Algorithm with Radius Parameters $R = 0.5$ and 0.7 in pp Collisions at $\sqrt{s} = 7$ TeV". In: **Phys. Rev. D** 90 (2014), p. 072006. DOI: [10.1103/PhysRevD.90.072006](https://doi.org/10.1103/PhysRevD.90.072006). arXiv: [1406.0324](https://arxiv.org/abs/1406.0324) [hep-ex].
-  **Morad Aaboud et al.** "Measurement of the inclusive jet cross-sections in proton-proton collisions at $\sqrt{s} = 8$ TeV with the ATLAS detector". In: **JHEP** 09 (2017), p. 020. DOI: [10.1007/JHEP09\(2017\)020](https://doi.org/10.1007/JHEP09(2017)020). arXiv: [1706.03192](https://arxiv.org/abs/1706.03192) [hep-ex].



References III

-  **Vardan Khachatryan et al.** "Measurement and QCD analysis of double-differential inclusive jet cross sections in pp collisions at $\sqrt{s} = 8$ TeV and cross section ratios to 2.76 and 7 TeV". In: **JHEP** 03 (2017), p. 156. DOI: [10.1007/JHEP03\(2017\)156](https://doi.org/10.1007/JHEP03(2017)156). arXiv: [1609.05331 \[hep-ex\]](https://arxiv.org/abs/1609.05331).
-  **M. Aaboud et al.** "Measurement of inclusive jet and dijet cross-sections in proton-proton collisions at $\sqrt{s} = 13$ TeV with the ATLAS detector". In: **JHEP** 05 (2018), p. 195. DOI: [10.1007/JHEP05\(2018\)195](https://doi.org/10.1007/JHEP05(2018)195). arXiv: [1711.02692 \[hep-ex\]](https://arxiv.org/abs/1711.02692).
-  **Vardan Khachatryan et al.** "Measurement of the double-differential inclusive jet cross section in proton-proton collisions at $\sqrt{s} = 13$ TeV". In: **Eur. Phys. J. C** 76 (2016), p. 451. DOI: [10.1140/epjc/s10052-016-4286-3](https://doi.org/10.1140/epjc/s10052-016-4286-3). arXiv: [1605.04436 \[hep-ex\]](https://arxiv.org/abs/1605.04436).
-  **Serguei Chatrchyan et al.** "Search for Contact Interactions Using the Inclusive Jet p_T Spectrum in pp Collisions at $\sqrt{s} = 7$ TeV". In: **Phys. Rev. D** 87 (2013), p. 052017. DOI: [10.1103/PhysRevD.87.052017](https://doi.org/10.1103/PhysRevD.87.052017). arXiv: [1301.5023 \[hep-ex\]](https://arxiv.org/abs/1301.5023).
-  **Serguei Chatrchyan et al.** "Search for quark compositeness in dijet angular distributions from pp collisions at $\sqrt{s} = 7$ TeV". In: **JHEP** 05 (2012), p. 055. DOI: [10.1007/JHEP05\(2012\)055](https://doi.org/10.1007/JHEP05(2012)055). arXiv: [1202.5535](https://arxiv.org/abs/1202.5535).
-  **W.J. Stirling**. **Private communication**.
<http://www.hep.ph.ic.ac.uk/~wstirlin/plots/plots.html>. 2012.

References IV

-  V. Bertone et al. "xFitter 2.0.0: An Open Source QCD Fit Framework". In: **PoS DIS2017** (2018), p. 203. DOI: [10.22323/1.297.0203](https://doi.org/10.22323/1.297.0203). arXiv: [1709.01151 \[hep-ph\]](https://arxiv.org/abs/1709.01151).
-  S. Alekhin et al. "HERAFitter, open source QCD fit project". In: **Eur. Phys. J. C** **75** (2015), p. 304. DOI: [10.1140/epjc/s10052-015-3480-z](https://doi.org/10.1140/epjc/s10052-015-3480-z). arXiv: [1410.4412 \[hep-ph\]](https://arxiv.org/abs/1410.4412).
-  H. Abramowicz et al. "Combination of measurements of inclusive deep inelastic $e^\pm p$ scattering cross sections and QCD analysis of HERA data". In: **Eur. Phys. J. C** **75** (2015), p. 580. DOI: [10.1140/epjc/s10052-015-3710-4](https://doi.org/10.1140/epjc/s10052-015-3710-4). arXiv: [1506.06042 \[hep-ex\]](https://arxiv.org/abs/1506.06042).
-  Albert M Sirunyan et al. "Measurement of tt normalised multi-differential cross sections in pp collisions at $\sqrt{s} = 13$ TeV, and simultaneous determination of the strong coupling strength, top quark pole mass, and parton distribution functions". In: **Eur. Phys. J. C** **80** (2020), p. 658. DOI: [10.1140/epjc/s10052-020-7917-7](https://doi.org/10.1140/epjc/s10052-020-7917-7). arXiv: [1904.05237 \[hep-ex\]](https://arxiv.org/abs/1904.05237).
-  Armen Tumasyan et al. "Measurement and QCD analysis of double-differential inclusive jet cross sections in proton-proton collisions at $\sqrt{s} = 13$ TeV". In: (Nov. 2021). arXiv: [2111.10431 \[hep-ex\]](https://arxiv.org/abs/2111.10431).
-  Torbjörn Sjöstrand et al. "An introduction to PYTHIA 8.2". In: **Comput. Phys. Commun.** **191** (2015), p. 159. DOI: [10.1016/j.cpc.2015.01.024](https://doi.org/10.1016/j.cpc.2015.01.024). arXiv: [1410.3012 \[hep-ph\]](https://arxiv.org/abs/1410.3012).

References V

-  Richard D. Ball et al. "Parton distributions with LHC data". In: **Nucl. Phys. B** 867 (2013), p. 244. DOI: [10.1016/j.nuclphysb.2012.10.003](https://doi.org/10.1016/j.nuclphysb.2012.10.003). arXiv: [1207.1303 \[hep-ph\]](https://arxiv.org/abs/1207.1303).
-  Vardan Khachatryan et al. "Event generator tunes obtained from underlying event and multiparton scattering measurements". In: **Eur. Phys. J. C** 76 (2016), p. 155. DOI: [10.1140/epjc/s10052-016-3988-x](https://doi.org/10.1140/epjc/s10052-016-3988-x). arXiv: [1512.00815 \[hep-ex\]](https://arxiv.org/abs/1512.00815).
-  Johan Alwall et al. "MadGraph 5 : going beyond". In: **JHEP** 06 (2011), p. 128. DOI: [10.1007/JHEP06\(2011\)128](https://doi.org/10.1007/JHEP06(2011)128). arXiv: [1106.0522 \[hep-ph\]](https://arxiv.org/abs/1106.0522).
-  J. Alwall et al. "The automated computation of tree-level and next-to-leading order differential cross sections, and their matching to parton shower simulations". In: **JHEP** 07 (2014), p. 079. DOI: [10.1007/JHEP07\(2014\)079](https://doi.org/10.1007/JHEP07(2014)079). arXiv: [1405.0301 \[hep-ph\]](https://arxiv.org/abs/1405.0301).
-  M. Bahr et al. "Herwig++ physics and manual". In: **Eur. Phys. J. C** 58 (2008), p. 639. DOI: [10.1140/epjc/s10052-008-0798-9](https://doi.org/10.1140/epjc/s10052-008-0798-9). arXiv: [0803.0883 \[hep-ph\]](https://arxiv.org/abs/0803.0883).
-  J. Pumplin et al. "New generation of parton distributions with uncertainties from global QCD analysis". In: **JHEP** 07 (2002), p. 012. DOI: [10.1088/1126-6708/2002/07/012](https://doi.org/10.1088/1126-6708/2002/07/012). arXiv: [hep-ph/0201195 \[hep-ph\]](https://arxiv.org/abs/hep-ph/0201195).

References VI

-  **Stefan Schmitt.** "TUnfold: an algorithm for correcting migration effects in high energy physics". In: **JINST** 7 (2012), T10003. DOI: 10.1088/1748-0221/7/10/T10003. arXiv: 1205.6201 [physics.data-an].
-  **Stefan Schmitt.** "Data Unfolding Methods in High Energy Physics". In: **EPJ Web Conf.** 137 (2017), p. 11008. DOI: 10.1051/epjconf/201713711008. arXiv: 1611.01927 [physics.data-an].
-  **Patrick L. S. Connor and Radek Žlebčík.** "Step: a tool to perform tests of smoothness on differential distributions based on Chebyshev polynomials of the first kind". In: (Nov. 2021). arXiv: 2111.09968 [hep-ph].
-  **CMS Collaboration and Thomas Mc Cauley.** "Displays of an event with two jets with transverse momentum of more than 3 TeV as seen in the CMS detector". **CMS Collection.** 2021. URL: <https://cds.cern.ch/record/2775841>.
-  **Sayipjamal Dulat et al.** "New parton distribution functions from a global analysis of quantum chromodynamics". In: **Phys. Rev. D** 93 (2016), p. 033006. DOI: 10.1103/PhysRevD.93.033006. arXiv: 1506.07443 [hep-ph].
-  **Richard D. Ball et al.** "Parton distributions from high-precision collider data". In: **Eur. Phys. J. C** 77 (2017), p. 663. DOI: 10.1140/epjc/s10052-017-5199-5. arXiv: 1706.00428 [hep-ph].

References VII

-  L. A. Harland-Lang et al. "Parton distributions in the LHC era: MMHT 2014 PDFs". In: **Eur. Phys. J. C** 75 (2015), p. 204. DOI: [10.1140/epjc/s10052-015-3397-6](https://doi.org/10.1140/epjc/s10052-015-3397-6). arXiv: [1412.3989 \[hep-ph\]](https://arxiv.org/abs/1412.3989).
-  S. Alekhin et al. "Parton distribution functions, α_s , and heavy-quark masses for LHC Run II". In: **Phys. Rev. D** 96 (2017), p. 014011. DOI: [10.1103/PhysRevD.96.014011](https://doi.org/10.1103/PhysRevD.96.014011). arXiv: [1701.05838 \[hep-ph\]](https://arxiv.org/abs/1701.05838).
-  Xiaohui Liu, Sven-Olaf Moch, and Felix Ringer. "Phenomenology of single-inclusive jet production with jet radius and threshold resummation". In: **Phys. Rev. D** 97 (2018), p. 056026. DOI: [10.1103/PhysRevD.97.056026](https://doi.org/10.1103/PhysRevD.97.056026). arXiv: [1801.07284 \[hep-ph\]](https://arxiv.org/abs/1801.07284).
-  J Currie, E. W. N. Glover, and J Pires. "Next-to-Next-to Leading Order QCD Predictions for Single Jet Inclusive Production at the LHC". In: **Phys. Rev. Lett.** 118 (2017), p. 072002. DOI: [10.1103/PhysRevLett.118.072002](https://doi.org/10.1103/PhysRevLett.118.072002). arXiv: [1611.01460 \[hep-ph\]](https://arxiv.org/abs/1611.01460).
-  James Currie et al. "Single Jet Inclusive Production for the Individual Jet p_T Scale Choice at the LHC". In: **Acta Phys. Polon. B** 48 (2017), p. 955. DOI: [10.5506/APhysPolB.48.955](https://doi.org/10.5506/APhysPolB.48.955). arXiv: [1704.00923 \[hep-ph\]](https://arxiv.org/abs/1704.00923).
-  Thomas Gehrmann et al. "Jet cross sections and transverse momentum distributions with NNLOJET". In: **PoS RADCOR2017** (2018). Ed. by Andre Hoang and Carsten Schneider, p. 074. DOI: [10.22323/1.290.0074](https://doi.org/10.22323/1.290.0074). arXiv: [1801.06415 \[hep-ph\]](https://arxiv.org/abs/1801.06415).

Patrick L.S. CONNOR

Universität Hamburg

<https://www.desy.de/~connorpa>

Institut für Experimentalphysik

Tel.: +49 40 8998-2617

Geb.: DESY Campus 68/121

Center for Data Computing and natural Sciences

Tel.:

Geb.: Notkestraße 9

